Performance Analysis of Beam-Switching using One-Dimensional Antenna Arrays

Manuel Lobinger, Kevin Niederwanger, Stefan Schwarz
Institute of Telecommunications, TU Wien, Austria
Christian Doppler Laboratory for Dependable Wireless Connectivity for the Society in Motion

***Abstract*—Adaptive beamforming (BF) is a well known application of active BF but comes with the cost of high complexity and computational effort in terms of angle and channel estimation. In order to find a low complexity alternative of adaptive BF we investigate the performance of a beam-switching method considering a uniform linear antenna array (ULA), one dimensional BF and two-wave with diffuse power (TWDP) fading. Therefore we compare adaptive BF with analog BF considered as beam-switching using horizontally and vertically arranged ULAs in terms of signal-to-noise ratio (SNR) and achievable rate by means of Monte Carlo simulations.**

***Index Terms*—Fading, TWDP, Beam Alignment, Beam-Switching, Beamforming, TWDP fading, Antenna Arrays**

I. Introduction

The increasing demand of network connectivity is a huge challenge for wireless service providers. On the one hand they try to improve the quality of service for mobile costumers, but on the other hand they want to keep their expenses low. LTE Release 14 provided the standardisation of full-dimensional MIMO and enabled active beamforming (BF) with a uniform linear antenna array (ULA) for base stations [1]–[3]. Adaptive BF for mobile users requires significant overhead for channel state information (CSI) estimation, such as estimation of signal angles of arrival/departure, furthermore each antenna needs an expensive radio frequency (RF) chain and power amplifier, therefore an adaptive BF strategy is cost intensive and complex. This can be reduced significantly with analog BF, where only one RF chain and power amplifier is needed. In this paper we compare such adaptive BF with a beam-switching strategy, where the base station/transmitter decides dependent on the position of the user which fixed beam of a given number of possibilities is the best. Our focus thereby is on vehicle-to-infrastructure (V2I) communications scenarios, were we investigate a user moving on a straight line, simulating a street, highway or railway, comparing signal-to-noise ratio (SNR) and average achievable rate along the path. Such a scenario is well-suited for a beam-switching approach, since the users move along well-defined trajectories. Due to the similarities to a railroad vehicle-to-infrastructure scenario, we consider two-wave with diffuse power (TWDP) fading [5]–[9], which is well suited according to [10], [11].

II. Channel Model

In this section we describe the fading model, computation of the SNR and achievable rate. We consider a single base station (BS) with a one dimensional ULA consisting of N_t isotropic antenna elements attached. A single user with an omnidirectional receive antenna is moving along the y-axis in a 3D coordinate system, as illustrated in Fig. 1.

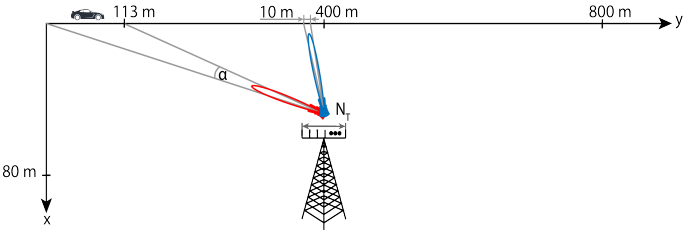

Fig. 1. An example beamwidth α of 8.6 degree with a horizontally aligned ULA reaches two different lengths of the path depending on the steering angle.

The array steering vector of a ULA $\mathbf{a}(\theta) \in \mathbb{C}^{N_t \times 1}$ can be expressed as

$$\mathbf{a}(\theta) = [1, \exp(j2\pi d/\lambda \sin(\theta), \ldots, \exp(j2\pi d/\lambda \sin(\theta)(N_t - 1)]^T, \quad (1)$$

where θ can be the azimuth or the elevation angle dependent on the alignment of the ULA. λ is the wavelength and d is the spacing between the array elements.

In our channel model we consider a line-of-sight (LOS) component represented by the angle θ_{LOS} and a dominant ground reflection represented by the angle θ_R. Additional we consider weaker multipath components by a diffuse scattering part represented by a complex Gaussian random vector $\mathbf{x}$, $\mathbf{y} \in \mathbb{C}^{N_t \times 1} \sim \mathcal{N}(\mathbf{0}, \sigma^2 \mathbf{I}_{N_t})$. This leads to a MISO TWDP fading channel

$$\mathbf{h}(y) = V_1 \mathbf{a}(\theta_{LOS}) + V_2 \mathbf{a}(\theta_R) e^{-j(\phi_d + \phi_r)} + \mathbf{x} + j\mathbf{y}, \quad (2)$$

with the parameters

$$K = \frac{{V_1}^2 + {V_2}^2}{2\sigma^2}, \quad \Delta = \frac{2V_1V_2}{{V_1}^2 + {V_2}^2}, \quad (3)$$

where V_1 and V_2 are constant amplitudes of the specular components. The K-factor is the power ratio of the specular components to the diffuse component. The power of the diffuse component is given by the variance σ^2. The Δ parameter is a relationship between the amplitudes of the specular

components. ϕ_d is a phase shift due to the longer propagation path of the ground reflection and the random phase shift $\phi_r \in \{0, \pi\}$ models a phase difference between the specular components due to the reflection. Because we are using a one-dimensional ULA the angles θ_{LOS} and θ_R of (2) need to be defined corresponding to the array alignment. For a vertically aligned ULA the angles are defined as

$$\theta_{LOS} = \arctan\left(\frac{r_z}{\sqrt{r_x^2 + r_y^2}}\right), \tag{4}$$

$$\theta_R = \arctan\left(\frac{r_z - 2h_r}{\sqrt{r_x^2 + r_y^2}}\right), \tag{5}$$

and for a horizontally aligned ULA as

$$\theta_{LOS} = \theta_R = \arctan\left(\frac{r_y}{r_x}\right), \tag{6}$$

with the vector from the base station to the user

$$\mathbf{r} = \begin{bmatrix} r_x \\ r_y \\ r_z \end{bmatrix}, \tag{7}$$

and the receive antenna height h_r.

III. Beam-Switching

The beam-switching method can be realised with a piece-wise defined precoder

$$\mathbf{f}(y) = \begin{cases} \mathbf{f}_1 = \frac{1}{\sqrt{N_t}}\mathbf{a}(\theta_1), & y_{d_0} \le y < y_{d_1} \\ \mathbf{f}_2 = \frac{1}{\sqrt{N_t}}\mathbf{a}(\theta_2), & y_{d_1} \le y < y_{d_2} \\ \quad\vdots & \quad\vdots \\ \mathbf{f}_n = \frac{1}{\sqrt{N_t}}\mathbf{a}(\theta_N), & y_{d_{N-1}} \le y < y_{d_N} \end{cases}, \tag{8}$$

where N is the number of used beams and θ_i is the angle of the i-th beam pointing somewhere between the decision boundaries $y_{d_{i-1}}$ and y_{d_i}. All angles θ_i only depend on the y-coordinate, because the x distance is constant. Have in mind that all θ_i can be elevation or azimuth angles dependent on the alignment of the used ULA.

IV. Adaptive Beamforming

We compare the simulation results from the beam-switching method with adaptive BF as an optimal BF strategy, therefore it is necessary to fully define the adaptive method as well. The precoder in this case can be defined as

$$\mathbf{f}_a(y) = \frac{1}{\sqrt{N_t}}\mathbf{a}(\theta_{LOS}), \tag{9}$$

with θ_{LOS} defined in (4) or (6), which always leads to a beam towards the user.

V. Optimization

To make a comparison of the whole scenario possible, we chose to look at the average achievable rate

$$R = \frac{1}{L}\int_{\mathscr{Y}} B \cdot \log_2\left(1 + \mathrm{SNR}(y)\right) dy, \tag{10}$$

with the length L of the given path $\mathscr{Y}$ and the bandwidth B. The corresponding SNR of the user is calculated by

$$\mathrm{SNR}\,(y) = \frac{P\,\xi^{-1}\,|\mathbf{h}(y)^H\mathbf{f}(y)|^2}{\sigma_N^2}, \tag{11}$$

where σ_N^2 is the variance of the noise, i.e. thermal noise and the noise figure from the user equipment. P is the transmit power and the path loss ξ is defined by

$$\xi = \left(\frac{4\pi D}{\lambda}\right)^{\alpha}, \tag{12}$$

with the distance D between the user and the BS, the wavelength λ and the path loss exponent α. For the best overall performance an optimization problem for maximizing the average achievable rate can be formulated as

$$\max_{\phi_i \in \mathbf{\Phi}, y_{d_i} \in \mathbf{D}} \frac{1}{L}\int_{\mathscr{Y}} B \cdot \log_2(1 + \mathrm{SNR}(y))dy, \tag{13}$$

where $\mathbf{D}$ is the set of decision boundaries $\{y_{d_0}, \ldots, y_{d_N}\}$ and $\mathbf{\Phi}$ is the beamset $\{\phi_1, \ldots, \phi_N\}$. This optimization has some difficulties. With a low beam count one has to find the beam directions, which result in the highest achievable rate. It is not that easy as it may sound, due to the geometry. Depending on the distance between the BS and the user one beam covers more or less distance of the path. In Fig. 1 an example beamwidth of 8.6 degree results in $10\,\mathrm{m}$ in the middle but in $113\,\mathrm{m}$ at the beginning of the path. However, the path loss increases with distance. With a high number of beams available searching for the optimal directions and boundaries gets difficult because of the high count of variables. To present some reasonable results without solving this optimization explicitly we decided to look on the performance of uniformly distributed decision boundaries, where every beam is pointing to the center of two boundaries.

VI. Simulation Setup

This section describes the simulation scenario, especially the geometry and simulation parameters. As mentioned in Section I we simulate one user moving on a straight line. The user starts at the origin and moves along the y-axis to $y = 800\,\mathrm{m}$. The BS is placed in the middle of the path in a distance of $x = 80\,\mathrm{m}$ and the antenna is placed at a height of $z = 32\,\mathrm{m}$. With this placement the azimuth angle from the BS to the user reaches ± 78.69 degree and the elevation angle ± 15.36 degree. We compare the results for a vertically and a horizontally arranged ULA using beam-switching with their limit of adaptive BF. For the beam-switching we distribute the fixed beams uniformly over the represented angle of the used ULA, but not exactly in the same way for both cases,

this will be explained in Section VII. All simulations are done with our 5G System Level Simulator [4]. The main simulation parameters are summarized in Table I.

TABLE I
SIMULATION PARAMETERS

Transmit power	$P = 1\,\mathrm{W}$
Path loss exponent	$\alpha = 2$
Carrier frequency	$2\,\mathrm{GHz}$
System bandwidth	$20\,\mathrm{MHz}$
Channel model	TWDP Fading, $\mathrm{K} = 10$, $\Delta = 0.98$, $V_1 = 1$
Antenna configuration	ULA with 16 Elements
Antenna spacing	$d = \frac{\lambda}{2}$

VII. Simulation Results

In this section we discuss and analyse numerical results from our simulations of the horizontal and vertical ULA.

A. Horizontal ULA

Fig. 2 shows the achievable SNR on the given path for adaptive BF and beam-switching. The curve for the adaptive BF shows clearly the fading due to the TWDP model. With beam-switching there are some spots, where the performance is quite low compared to the adaptive BF. These deep fades occur because of the sharp beamwidth and there are not enough beams to cover these areas. Also noticeable is that the weak performance spots are concentrated in the middle. This is caused by the geometry of our scenario, namely, beams closer to the end of the path on both sides cover more distance, although the beamwidth stays the same. Fig. 3 shows the average achievable rate for different numbers of beams. By increasing the number of beams the achievable rate slowly approaches the limit of adaptive BF. Starting with one beam with an achievable rate of $186.6\,\mathrm{MBit/s}$, which is a loss of 42.66 percent, reaching an achievable rate of $314.8\,\mathrm{MBit/s}$ with eleven beams, resulting in a loss of 2.66 percent. With these numerical results shown the beam-switching method gets close to adaptive BF when a high number of beams is used, although a few performance holes in the SNR occur.

B. Vertical ULA

In Fig. 4 we see a remarkable result. The SNR over the path for the beam-switching method with five beams is almost identical with the adaptive BF. Fig. 5 is again a plot for the average achievable rate showing the growth in performance over the number of beams. With only one beam the system reaches an average achievable rate of $270.6\,\mathrm{MBit/s}$, which is a loss of 15.75 percent compared with the maximal performance. With four beams the performance loss decreases to 0.44 percent. Compared to a horizontal array this version reaches the limit faster and has a better performance at lower number of beams. This behaviour is due to the one dimensional antenna array. With only vertically arranged antenna elements the beam pattern is not dependent on the azimuth angle and covers the entire horizontal plane. This leads to a beam, which covers a circle around the BS with a radius dependent on the height of

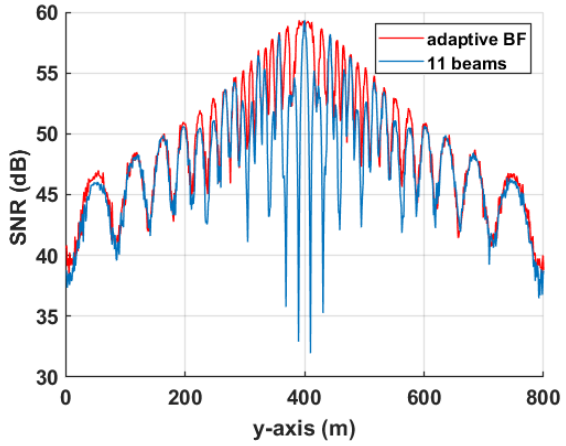

Fig. 2. SNR for adaptive BF and beam-switching with a horizontal ULA and 11 uniformly distributed fixed beams.

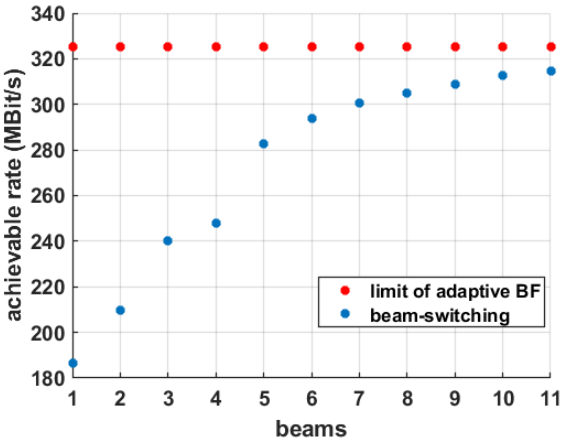

Fig. 3. Achievable rate for beam-switching with a horizontal ULA compared to the limit from adaptive BF.

the antenna and the elevation of the used BF. This creates in our scenario a symmetry plane at $y = 400\,\mathrm{m}$. This means every beam facing a position between $0\,\mathrm{m}$ and $400\,\mathrm{m}$ on the y-axis is automatically a useful beam at the corresponding distance between $400\,\mathrm{m}$ and $800\,\mathrm{m}$. The same behaviour applies for the horizontal array but the symmetry is on a vertical plane and is therefore not useful for our scenario. As previously mentioned the distribution of the beams is slightly different than in the horizontal case. Here the uniform distribution is only over half of the path because of the symmetry. Have in mind that although a smaller amount of beams is needed for the same performance, the number of beam switches over the whole path stays the same. The advantage here is that one beam is used for two different positions. Although this behaviour could be a disadvantage when considering interference in a multi user and/or multi base station scenario, which will be investigated in future work.

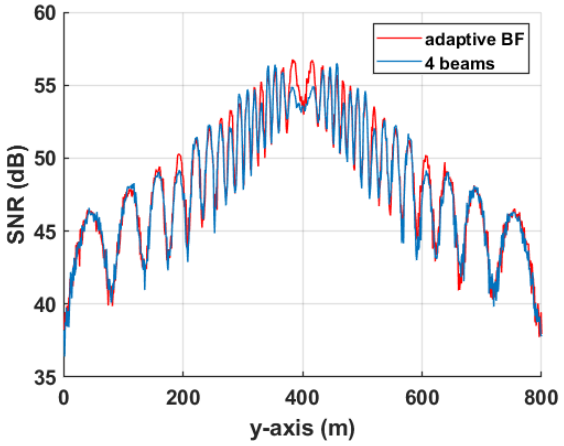

Fig. 4. SNR for adaptive BF and beam-switching with a vertical ULA and 4 uniformly distributed fixed beams.

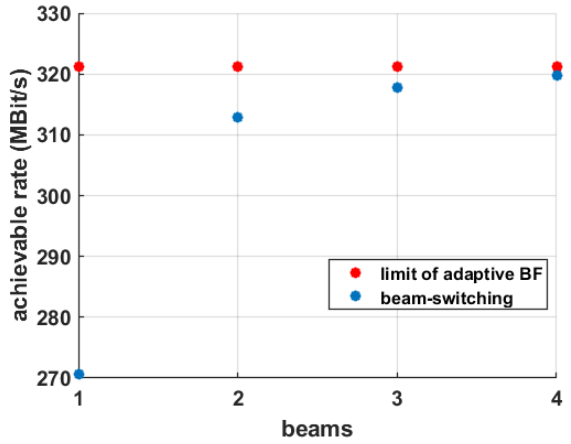

Fig. 5. Achievable rate for beam-switching with a vertical ULA compared to the limit from adaptive BF.

VIII. Conclusion

The proposed beam-switching model was analyzed and simulated with a horizontally and a vertically arranged ULA. The results show that even without an optimization of the beam distribution, beam-switching with uniformly distributed beams and a vertical ULA approaches the performance of an adaptive BF strategy with a small set of four beams. The horizontal ULA could reach the limits of adaptive BF but needs a far bigger beamset to achieve this. In our future work, we will consider two-dimensional antenna arrays, as well as, the interference between multiple users and base stations.

Acknowledgment

The financial support by the Austrian Federal Ministry for Digital and Economic Affairs and the National Foundation for Research, Technology and Development is gratefully acknowledged.

References

[1] H. Ji et al., "Overview of Full-Dimension MIMO in LTE-Advanced Pro," in IEEE Communications Magazine, vol. 55, no. 2, pp. 176-184, February 2017.

[2] Y. Nam et al., "Full dimension MIMO for LTE-Advanced and 5G," 2015 Information Theory and Applications Workshop (ITA), San Diego, CA, 2015, pp. 143-148.

[3] 3GPP TR 36.897, "Study on Elevation Beamforming/Full-Dimension (FD) MIMO for LTE".

[4] M. Müller et al., "Flexible multi-node simulation of cellular mobile communications: the Vienna 5G System Level Simulator," in EURASIP Journal on Wireless Communications and Networking, 10.1186/s13638-018-1238-7, 2018.

[5] J. P. Peña-Martín, J. M. Romero-Jerez and F. J. Lopez-Martinez, "Generalized MGF of the Two-Wave With Diffuse Power Fading Model With Applications," in IEEE Transactions on Vehicular Technology, vol. 67, no. 6, pp. 5525-5529, June 2018.

[6] E. Zöchmann et al., "Better than Rician: modelling millimetre wave channels as two-wave with diffuse power," J. Wireless Com Network 2019.

[7] S. Schwarz and E. Zöchmann, "Robust Beam-Alignment for TWDP Fading Millimeter Wave Channels," in IEEE 20th International Workshop on Signal Processing Advances in Wireless Communications (SPAWC), Cannes, France, 2019, pp. 1-5., 2019.

[8] J. Moreno, J. M. Riera, L. d. Haro and C. Rodriguez, "A survey on future railway radio communications services: challenges and opportunities, " in IEEE Communications Magazine, vol. 53, no. 10, pp. 62-68, October 2015.

[9] S. Schwarz, T. Philosof and M. Rupp, "Signal Processing Challenges in Cellular-Assisted Vehicular Communications: Efforts and developments within 3GPP LTE and beyond, " in IEEE Signal Processing Magazine, vol. 34, no. 2, pp. 47-59, March 2017.

[10] E. Zöchmann, J. Blumenstein, R. Marsalek, M. Rupp and K. Guan, "Parsimonious Channel Models for Millimeter Wave Railway Communications, "2019 IEEE Wireless Communications and Networking Conference (WCNC), Marrakesh, Morocco, 2019, pp. 1-6.

[11] H. Groll et al., "Sparsity in the Delay-Doppler Domain for Measured 60 GHz Vehicle-to-Infrastructure Communication Channels, " 2019 IEEE International Conference on Communications Workshops (ICC Workshops), Shanghai, China, 2019, pp. 1-6.